Project Number 282910

ÉCLAIRE

Effects of Climate Change on Air Pollution Impacts and Response Strategies for European Ecosystems

Seventh Framework Programme

Theme: Environment

D4.3 – A Coupled Pollutant Deposition and Carbon Based Growth Model

Due date of deliverable: **31/10/2014**   Actual submission date: **03/11/2014**

Start Date of Project: **01/10/2011**   Duration: **48 months**

Organisation name of lead contractor for this deliverable :
Stockholm Environment Institute-York, University of York

	Project co-funded by the European Commission within the Seventh Framework Programme	
	Dissemination Level	
PU	Public	X
PP	Restricted to other programme participants (including the Commission Services)	☐
RE	Restricted to a group specified by the consortium (including the Commission Services)	☐
CO	Confidential, only for members of the consortium (including the Commission Services)	☐

1. Executive Summary

This deliverable provides details of a new module that has been developed for use within the DO_3SE modelling scheme that enables the estimation of both total ozone deposition and stomatal ozone uptake assuming a coupling between stomatal conductance (g_{sto}) and net photosynthesis (A_{net}). This allows stomatal ozone uptake to be closely related to three processes that are considered primarily responsible for limiting A_{net}: (i) Rubisco activity (A_c), (ii) the regeneration of ribulose-1,5-bisphosphate (RuBP) which is limited by the rate of electron transport (A_j), and (iii) an inadequate rate of transport of photosynthetic products (most commonly triose phosphate utilization). The rate of A_{net} will determine the demand for CO_2 which in turn is considered to feedback onto the CO_2 supply which is determined by g_{sto}. Theory suggests that g_{sto} will vary to ensure that an optimum supply of CO_2 is provided which at the same time limits H_2O vapour loss from the plant.

This theory is brought into the DO_3SE model by incorporating the formulations of Farquhar et al. (1980), which allow the estimate of A_{net} according to biochemical processes; the core 'Farquhar' model is updated with new and additional formulations that are described in the scientific literature and have shown improvements in the estimation of A_{net} for a range of conditions and species. The coupling between A_{net} and g_{sto} is achieved using the methods first developed by Ball et al. (1987) who discovered an empirical linear relationship, which relates g_{sto} to a combination of A_{net} and environmental parameters, such as leaf surface relative humidity (D_h) and CO_2 concentration (C_a). Again, this core method has been updated to ensure that the most recent developments that improve simulations of g_{sto} in relation to A_{net} are included (i.e. use of (i) CO_2 concentration at the leaf surface, (ii) methods that account for the CO_2 compensation point and (iii) vapour pressure deficit rather than D_h).

The new module also incorporates new methods to estimate the instantaneous effect of ozone on this Anet-gsto configuration. These rely on the fact that ozone damages the plants maximum carboxylation rate (Vcmax), supported by the literature (see datamining exercise conducted in WP9). A unique aspect of this new module is that it allows for recovery of Vcmax, this will be particulary important when applying the model to real world conditions (i.e. where ozone is episodic rather than the more continuous elevated ozone exposures applied in experimental fumigation studies). The resulting A_{net} - g_{sto} module, with ozone damage function, has been incorporated into the DO_3SE model framework (essentially substituting the previous g_{sto} module, which used a multiplicative model to estimate g_{sto} based on Jarvis, 1976). The model is currently being used with ECLAIRE experimental data collected in C3, WP10 and WP11 to help analyse the experimental data as well as to evaluate certain aspects of the model (e.g. its capacity to simulate key plant physiological variables such as An and leaf temperature).

The model has been parameterised for European land cover types, consistent with those used by the EMEP model. This has required the identification from the literature of 5 parameter values for 9 landcover types made up of 11 different species. Finally, the model has been coded so as to allow easy incorporation into the ESX modelling scheme.

Objectives:

To improve an existing ozone deposition model (DO$_3$SE, Deposition of Ozone for Stomatal Exchange) through

1. development of model algorithms to incorporate photosynthetic based estimates of stomatal conductance to improve the stomatal and non-stomatal estimate of total deposition;
2. to incorporate a feedback effect of ozone on stomatal conductance;
3. parameterisation of the model for application across Europe within the EMEP model and;
4. a model formulation coded so as to be easily available for use in EMEP (the ESX model).

2. Activities:

- Literature review to identify most appropriate algorithms for incorporation into new A_{net}-g_{sto} module that is fundamentally based on Farquhar et al. (1980) and Ball et al. (1987).
- Literature review to identify the most appropriate mechanism by which an ozone feedback can be bought into the model.
- Literature review to parameterise the model for European conditions.
- Work on programming the code to identify the mechanisms by which these algorithms can be incorporated into the ESX model framework.

3. Results:

- Identification of the algorithms that will together form the new A_{net}-g_{sto} module
- Identification of a method to incorporate the influence of ozone (and nitrogen) on photosynthesis and stomatal conductance
- Parameterisation of the model for European land cover types
- Coding of the new algorithms into the existing DO$_3$SE model (substituting the existing multiplicative algorithms)

4. Milestones achieved:

MS 15: Literature review on the effects of ozone and nitrogen deposition on stomatal functioning.
MS 17: Improved representation of the influence of environmental drivers on stomatal conductance

5. Deviations and reasons:

None

6. Publications:

None

7. Meetings:

None

8. List of Documents/Annexes:

A coupled pollutant and carbon based growth model

1. Coupled photosynthesis-stomatal conductance model (A_{net}-g_{sto})

The objective of the coupled photosynthesis-stomatal conductance model (A_{net}-g_{sto}) model is to quantify leaf or canopy scale g_{sto} with the help of easily accessible environmental parameters such as air temperature (T_{air}), ambient CO_2 concentration (c_a) and irradiance (PAR). The A_{net}-g_{sto} model consists of a combination of two separate models, whose main components are outlined below and include i. the empirical A_{net}-g_{sto} model that estimates g_{sto} (Leuning, 1990) and ii. the mechanistic and biochemical Farquhar model (Farquhar et al., 1980) that estimates net carbon assimilation or net phostosynthesis (A_{net}).

One of the first coupled A_{net}-g_{sto} models was that published by (Leuning, 1990), though some other authors are often cited as the originating sources of the model (e.g. Collatz et al., 1991 and Harley et al., 1992). The models they apparently developed independently are essentially equivalent. The order of description of the A_{net}-g_{sto} modelling here follows the order in which they have to be computed.

2. Biochemical Farquhar model for net photosynthesis (A_{net})

The underlying assumption to Farquhars's 1980 model is that, according to prevailing environmental conditions, either rubisco activity (A_c) or the regeneration of ribulose-1,5-bisphosphate (RuBP), which is limited by the rate of electron transport (A_j), limits photosynthesis. Subsequent to Farquhar's 1980 paper, Harley et al. (1992) identified a third limitation resulting from inadequate rate of transport of photosynthetic products (most commonly this is due to triose phosphate utilization) (A_p). This limit has now become standard in many models of A_{net} (e.g. Sellers et al., 1996; Cox et al., 1999) and is included here. Taking these influences on photosynthesis into account, A_{net} is calculated by determination of the smaller of these theoretical CO_2 assimilation rates, less the rate of dark respiration (R_d) (Farquhar et al., 1980) as in eq. 1 and as described in Figure 1.

$$A_{net} = \min(A_c, A_j, A_p) - R_d \qquad\qquad 1$$

Figure 1 Scheme showing some of the processes that affect photosynthetic rate. For each of the three panels, any process in that panel will cause the photosynthetic rate to vary with [CO_2] in the same way. From Sharkey et al. (2007).
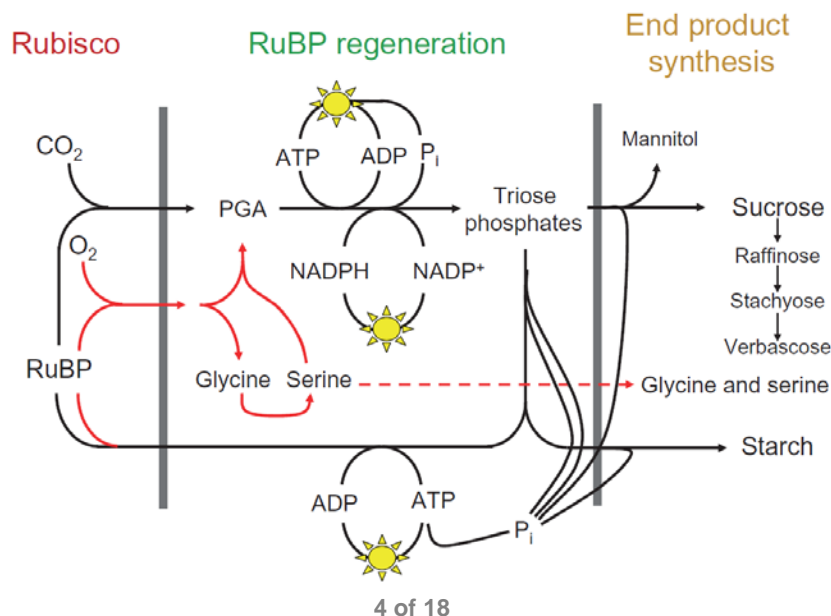
Within the literature there are small variations in the precise methods to estimate Ac, Aj and Ap. One important application of our A_{net}-g_{sto} model is that it is to be made with empirical data collected at sites across Europe. This provides the opportunity to use empirical data to parameterise the key components of the model. However, methods to perform this parameterisation should be consistent with these methods used to estimate A_{net}. Therefore our model will follow the eqs. recently described by Sharkey et al. (2007), since these are expected to represent both the most recent formulations as well as those that are consistent with the derivation of key parameters, described in more detail in section 3. The potential rate of assimilation limited only by Rubisco activity (A_c) is calculated according to Sharkey et al. (2007) as in eq 2.

$$A_c = V_{cmax} \left[\frac{c_i - \Gamma*}{c_i + K_c \cdot \left(1 + \frac{O_i}{K_o}\right)} \right] \qquad\qquad 2$$

Where V_{Cmax} is the maximum rate of Rubisco activity, c_i and O_i are intercellular concentrations of CO_2 and O_2 respectively, K_c and K_o are the Michaelis-Menten coefficients of Rubisco for CO_2 activity (in µmol mol^{-1}) and O_2 (in mmol mol^{-1}), respectively, and $\Gamma*$ is the CO_2 compensation point in the absence of mitochondrial (dark) respiration.

The potential rate of assimilation when RuBP regeneration is limiting is given in eq. 3.

$$A_j = J \; \frac{c_c - \Gamma*}{a.c_c + b.\Gamma*} \qquad\qquad 3$$

Where J is the electron transport rate and the parameters a and b denote the electron requirements for the formation of NADPH and ATP, respectively. The exact values differ slightly throughout the literature but are all close to $a = 4$ and $b = 8$ assuming four electrons per carboxylation and oxygenation (Sharkey et al., 2007). J is related to incident photosynthetically active photon flux density (Q) where the light response of a plants photosystem first follows a linear rise with an increase in radiation Q until it reaches an area of saturation where the electron transport rate J approaches its maximum value (J_{max}). Mathematically this is represented by the quadric relationship shown in eq. 4 after Leuning (1990).

$$J = \frac{(J_{max} + \propto Q) - \sqrt{(J_{max} + \propto Q)^2 - 4 \propto Q \emptyset J_{max}}}{2.\emptyset} \qquad\qquad 4$$

Where α is the quantum yield of electron transport, which determines the slope of the linear rise in the low irradiance regime, and Ø is the curvature of the light response curve normally acquired by experimental fitting. The value of α was fixed at 0.3 mol electrons mol^{-1} photon, based on an average C3 photosynthetic quantum yield of 0.093 and a leaf absorptance of 0.8 (cf. Medlyn et al., 2002). The value of Ø was taken to be 0.90 (Medlyn et al., 2002). These parameter values have only a slight effect on the estimated value of J_{max}.

Finally, the potential rate of assimilation when the utilization of triose phosphate is limiting assimilation (A_p) (i.e. when the chloroplast reactions have a higher capacity than the capacity of the leaf to use the products of the chloroplasts) is estimated rather simply by eq. 5 after Collatz et al. (1991).

$$A_p = 0.5 . V_{cmax} \qquad\qquad 5$$

The key parameters of the model J_{max} and V_{Cmax}, as well as the parameters K_c, K_o and $\Gamma*$, all vary with temperature (Medlyn et al., 2002). J_{max} and V_{Cmax} also vary between species, whilst K_c, K_o and $\Gamma*$are considered intrinsic properties of the Rubisco enzyme and therefore can be assumed constant between

species (Harley et al., 1986). Due to the temperature effects on the Rubisco enzyme, which catalyses the corresponding process, Γ* is temperature dependent as well.

The original model of Farquhar et al. (1980) used a purely empirical polynomial from Brooks & Farquhar (1985), which approximated the temperature dependence of these different parameters. Since then many studies have investigated these temperature dependencies more thoroughly; here we follow the rational of Medlyn et al. (2002) who advised using the temperature relationships provided by Bernacchi et al. (2001) who used an Arrhenius equation to describe the processes and based these functions on measurements made *in vivo* without disturbance of the leaf. The rate of dark respiration R_d, Γ* and the Michaelis-Menten constants for CO_2 and O_2 (K_c and K_o) are computed using the standard formulations described in eq 6 and 7.

$$P(T) = P_{T,Ref}.exp\left(\frac{\Delta H.(T-T_{ref})}{T_{ref}.R.T}\right) \qquad\qquad 6$$

$$P(T) = P_{T,Ref}.exp\left(\frac{\Delta H_a.(T-T_{ref})}{T_{ref}.R.T}\right).\frac{1+exp\left(\frac{T_{ref}\Delta S-\Delta H_d}{T_{ref}.R}\right)}{1+exp\left(\frac{T\Delta S-\Delta H_d}{T.R}\right)} \qquad\qquad 7$$

where P denotes the different quantities, ΔH is the activation energy, ΔHd is the deactivation energy and ΔS is entropy for the processes; values for each process follow those given in Bernacchi et al. (2001). In general this formula describes a normal Arrhenius equation modified to incorporate an inhibition term at high temperatures.

The parameters ΔH_a and ΔH_d (energy for activation or deactivation of the process) describe the shape of the response function. Their values are species dependent and have to be fitted to experimental laboratory datasets. Medlyn et al. (2002) give a review of experimental values, Leuning (2002) assesses uncertainties incorporated by using mean values and Wohlfahrt et al. (1999) quantifies the mistakes caused by a wrong parameterisation. The value of the two quantities at T = 25°C, $P_{T,ref}$, can be more easily determined *via* gas exchange measurements. Wullschleger (1993) reviewed several experimental datasets and reports a wide set of values for different species.

In summary, the Farquhar model mathematically quantifies a detailed mechanistic understanding of the biochemical processes in the chloroplasts which govern photosynthesis. It allows for the estimation and calculation of the CO_2 assimilation rate as a function of leaf temperature, irradiance and internal CO_2 concentration.

3. Coupled photosynthesis-stomatal conductance (A_{net}-g_{sto}) model.

Based on earlier observations of the constant ratio of g_{sto} to net CO_2 assimilation rate (A_{net}), Ball et al. (1987) discovered an empirical linear relationship, which relates g_{sto} to a combination of A_{net} and environmental parameters, such as leaf surface relative humidity (D_h) and CO_2 concentration (C_a) as shown in Figure 2.
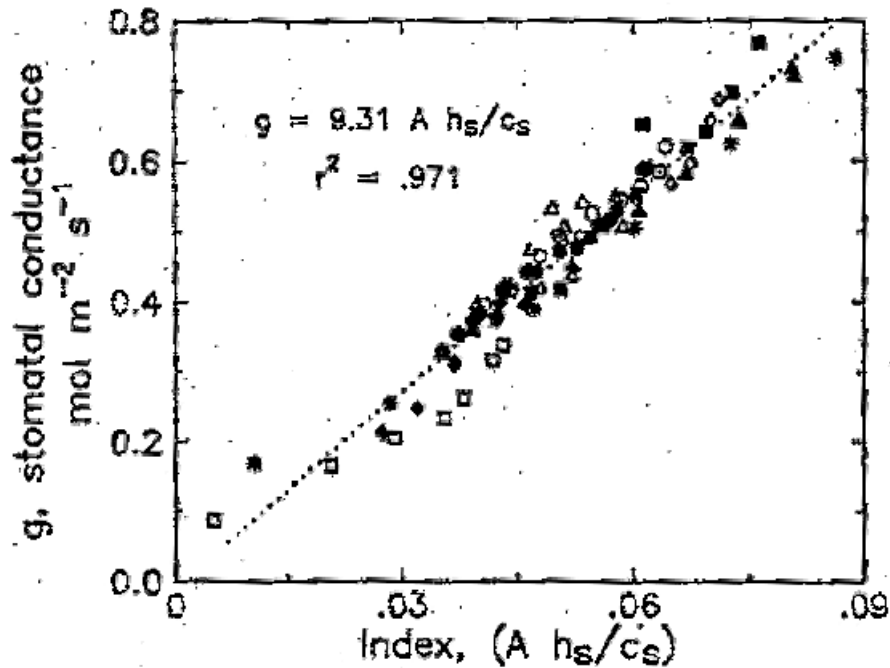

Figure 2. The original BWB model. Stomatal conductance plotted against the BWB Index. From Ball et al. (1987).

Leuning (1990 and 1995) modified the original Ball et al. (1987) relationship so that the function used leaf surface CO_2 concentration (C_s) less the CO_2 compensation point (Γ). They argued that the use of C_s rather than C_a (the CO_2 concentration outside the leaf boundary layer) eliminates complications arising from the transfer of CO_2 through the leaf boundary layer. The introduction of the Γ term allows the correct simulation of stomatal behaviour at low CO_2 concentrations which will tend towards zero as A_{net} becomes minimal close to the Γ. The use of humidity deficit (D_s) rather than relative humidity (D_h) accounts for the fact that stomates respond to humidity deficit rather than surface relative humidity. This response is actually mediated through leaf transpiration (Et_{leaf}), but the close link between Et_{leaf} and D_s means that the use of D_s is appropriate for simulations. Leuning (1995) found that a hyperbolic function for D_s provided an improved humidity response by accounting for the response of D_s to leaf temperature. The resulting formulation they propose is given in eq.8.

$$g_{sto} = g_0 + m.\frac{A_{net}}{[(c_s - \Gamma)(1 + D_s/D_0)]} \qquad \textbf{8}$$

The parameter g_0 is interpreted as the minimal g_{sto} (Leuning, 1990) and is equivalent to the intercept of the regression which is sometimes greater, but often close, to zero. The parameter m is the so called composite sensitivity of g_{sto} to assimilation rate and humidity/CO_2 concentration and can be obtained *via* a linear regression of g_{sto} against experimental data from steady state gas exchange measurements. The value of m is surprisingly consistent amongst many different species, and ranges between 5 and 15 (Kosugi et al., 2003) (if all quantities are in units consistent with Ball et al. (1987), m is dimensionless).

Despite the empirical and non-mechanistic nature of this model, it allows for the mathematical quantification of the key environmental feedbacks on stomatal behaviour: (1) Rising irradiance causes stomata to open (incorporated through the positive influence of radiation on A_{net}) until reaching the light compensation point; (2) Rising CO_2 causes stomata to close (incorporated through the negative influence of limited RuBP regeneration); (3) To minimize water loss, stomata close when the transpiration rate rises (incorporated through the response to leaf surface humidity deficit).

However, caution has to be exercised concerning interpretation of the model. It allows for no mechanistic explanation or causal interpretation of the feedbacks between the different parameters (see Aphalo & Jarvis (1993) for a discussion) and is, strictly speaking, only a statistical correlation.

4. Micrometeorological CO_2 supply model

It becomes clear that to calculate g_{sto}, the value of A_{net} is needed and for the calculation of A_{net} it is necessary to know g_{sto}. Baldocchi (1994) found an analytical solution for parts of the problem, and Su et al. (1996) and Nikolov et al. (1995) developed solutions for other sets of coupled equations. Still the vast majority of published models had to use numerical loops to iteratively guess values for different parameters that satisfy the different equations as the available analytic solutions are limited to certain sets of given environmental quantities and model formulations. An additional cross dependency is added to the model when T_{leaf} values have to be computed from T_{air}, as transpiration is a main driving force for leaf surface temperature control. Therefore g_{sto} is needed to calculate T_{leaf}, which can only be calculated when A_{net} is known and for this, again, T_{leaf} is needed (see Nikolov et al. (1995) for a solution).

To facilitate the calculation of the internal (C_i) and surface (Cs) CO_2 from ambient CO_2 concentrations (C_a), a boundary layer model equivalent to that used for calculating the exchange of O_3 across the same physical pathway is used. C_s is calculated as a function of C_a, A_{net} and g_b; C_i also requires an estimate of g_{sto}. These equations also follow those described in von Caemmerer & Farquhar (1981) and are as described in eq. 9 and 10.

$$c_s = c_a - A_{net} \cdot \frac{1.37}{g_b} \qquad\qquad\qquad\qquad \textbf{9}$$

$$c_i = c_a - A_{net} \frac{1.6\, g_b + 1.37 g_{sto}}{g_b \cdot g_{sto}} \qquad\qquad\qquad\qquad \textbf{10}$$

The g_b and g_{sto} conductance values are for water vapour and therefore eqs. 9 and 10 use the factors 1.6 and 1.37 (which are the ratios of the diffusivity of CO_2 and water vapour in still and semi turbulent air respectively).

Finally, the leaf surface humidity deficit D_s also has to be calculated. Firstly, the leaf surface relative humidity (h_s) is calculated as described in Nikolov et al. (1995) and eq. 11.

$$h_s = \frac{g_{sto} \cdot ei + g_b \cdot ea}{es\,(T_{leaf}) \cdot (g_{sto} + g_b)} \qquad\qquad\qquad\qquad 11$$

where ei is the water-vapor pressure in the intercellular air space of the leaf, es(T_{leaf}) is the saturation vapor pressure at leaf temperature and ea is the vapour pressure in the ambient air (all in Pa). This implies that the air inside the leaf boundary layer is at leaf temperature. In the case of a wet leaf, Eq. 11 does not apply because the air next to a wet surface is normally vapour-saturated and, therefore, $h_s = 1$.

D_s is then calculated using standard equations to convert relative humidity (here leaf surface relative humidity) into leaf to air vapour pressure deficits (here then leaf surface humidity deficit), which rely on temperature (here leaf temperature).

## 5.   Incorporation of the influence of ozone and leaf nitrogen on g_{sto}

This work has focussed on understanding how pollutant deposition (for ozone described as stomatal ozone flux, fO_3) might affect, and be affected by, key plant processes (this work has also benefited from close collaboration with the experimentalists in C3 in the ECLAIRE project). The means of incorporating photosynthesis (A) and stomatal conductance (g_{sto}) are described above and govern the balance between CO2 supply and demand (and thereby determine internal and supply CO_2 concentrations (Ci & Cs)). The rate of respiration (R) will then determine the rate of net photosynthesis (An) and the ultimate rate of C fixation. The latter will lead to alterations in biomass, yield and other types of damage. These core leaf level physiological interactions that occur between these different processes are described in Fig 3.

Fig 3. Connections between the different leaf level physiological processes that are affected by ozone and N deposition.
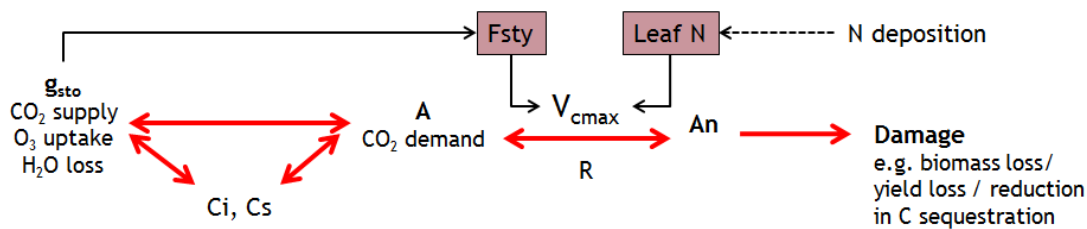
From Fig 3 it is clear that the maximum carboxylation capacity (Vcmax) is central, influencing both pollutant uptake and hence ozone deposition, as well as those processes that will determine damage. To accommodate this important aspect that controls ozone deposition the DO3SE model (now termed DO3SE_C or the An-gsto DO3SE) has been developed to incorporate a method that allows for an instantaneous assessment of ozone damage on gsto. This mechanism is based on a method described by (Martin et al., 2000) which modify the maximum carboxylation rate (Vcmax) according to the instantaneous ozone flux (Fsty) according to $\Delta Vcmax = k \cdot Fsty$ (see also Fig 4 where k= 2 and y = 2). Importantly, this method allows for the photosynthetic complex to recover when Fst values are below the y threshold.

Fig 4. The relationship between instantaneous ozone flux above a threshold 'y' (Fsty) and the % change in Vcmax.
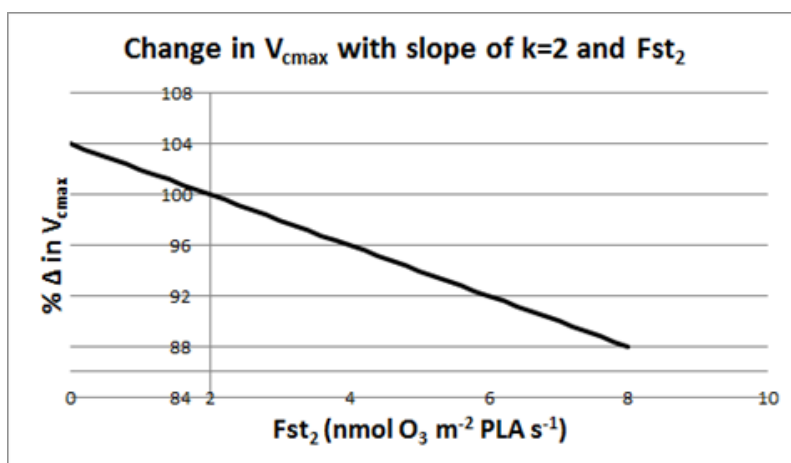
The development of this model provides an excellent opportunity to consider how combinations of pollutants act to influence leaf level plant physiology which will scale to canopy, stand and ultimately ecosystem level response. Tasks over the coming months will focus on evaluation of this method with ECLAIRE experimental data; this work will be conducted within C3. These methods can also be

introduced into the regional scale models used in C4 to bring consistency to the modelling methods used to assess the impacts of pollution on vegetation.

6.   Parameterisation of the new DO3SE_C model

A literature review was conducted to parameterise the new model. This review focussed on the following key model parameters:

Jmax - Maximum photosynthetic electron transport rate (a proxy for ribulose-1,5-bisphosphate regeneration)

Vcmax - Maximum carboxylation rate of Rubisco

m - Species-specific composite sensitivity of gs to An,

g0 – minimum stomatal conductance

All values taken from the literature were measurements made at $25^{o}C$ to ensure the values were not affected by temperature variation (Medlyn et al., 2002).

These parameters were found for 9 land cover types (denoted in bold in Table 1) and within these cover types, 11 species. These species and cover-types are those already defined by the EMEP photochemical model and the original, multiplicative DO3SE model. Therefore, this parameterisation gave consistency with the existing methods used to estimate deposition and stomatal ozone flux across Europe.

7.   Coding the new algorithms into the existing DO3SE model for availability to ESX.

The ESX model provides a new method of estimating atmospheric and in canopy exchange of pollutants. The ESX scheme is not based on resistances but relies on numerically solving diffusion equations for different pollutants with a parameterised exchange coefficient; essentially these equations replace the atmospheric and boundary layer resistances previously in the EMEP and DO_3SE models. The benefit of this unique approach is that these models are able to estimate both downward and upward flux of pollutants (i.e. can cope with pollutants that are both deposited to- as well as emitted from- vegetation such as ammonia (NH_3)).

The ESX model includes a layer-based canopy framework, numerical solutions to pollutant dispersal and the EMEPs model atmospheric chemistry algorithms. Each layer contains pollutant sources and sinks (e.g. due to presence of vegetation), has chemical interactions calculated within it, and is affected by dispersal between layers (see Figure 1; where z_i relates to pollutant mass transfer either as a source (z_i+1) or a sink (z_i-1) from a pollutant concentration defined at z_i). The model is designed to run over a short time step to work within EMEP's larger scale chemical transport model.

Figure 1.   A conceptualisation of the quantification of pollutant fluxes between layers within the ESX model.
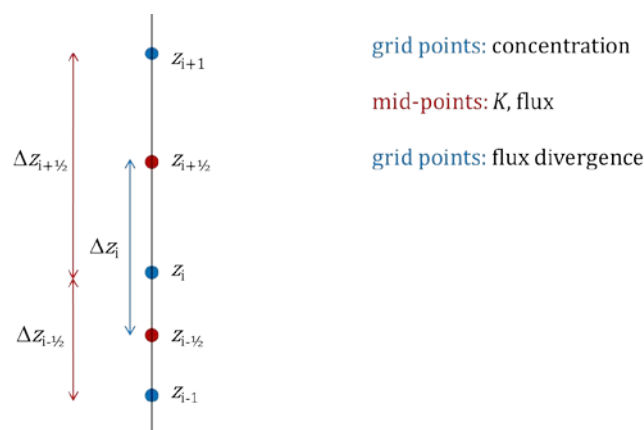
Table 1. Parameterisation of the DO3SE_C model – maximum carboxylation (Vcmax, μmol/m^2/s) and maximum photosynthetic electron transport rate (Jmax, μmol/m^2/s) (Jmax).

Species / cover type	Vcmax, μmol/m2/s (mean, median, range)	Ref	Jmax, μmol/m2/s (mean, median, range)	Ref
Deciduous forest	**56**	**N.B. JULES value is 36.8** (Clark et al., 2011)	**112**	
Birch	**51**, 57, [42-71]	Hayes, 2014 Pers. Comm. [57], Rey & Jarvis, 1998 [42], Dreyer, et al., 2001 [71]	**102**, 92, [84-125]	Hayes, 2014 Pers. Comm. [84], Rey & Jarvis, 1998 [92], Dreyer, et al., 2001 [125]
Beech	**52**, 52, [35-62]	Bader et al., 2010 [44], Löw et al., 2007 [62], Parelle et al., 2006 [50], Dreyer, et al., 2001 [66], Balandier et al., 2007 [35], Fleck, 2001 [55]	**107**, 107, [83-128]	Bader et al., 2010 [120], Löw et al., 2007 [113], Parelle et al., 2006 [98], Dreyer, et al., 2001 [128], Balandier et al., 2007 [83], Fleck, 2001 [100]
Temperate Oak	**65**, 69, [31-91]	Marzuoli & Gerosa (2014) Pers. Comm. [31], Dreyer et al., 2001 [88] & [91], Bader et al., 2010 [50]	**129**, 152, [57-157]	Marzuoli & Gerosa (2014) Pers. Comm. [57], Dreyer et al., 2001 [154] & [157], Bader et al., 2010 [150]
Coniferous forest	**79**	**N.B. JULES value is 26.4** (Clark et al., 2011)	**190**	
Norway spruce	**71**, 71, [60-81]	Zheng et al., 2002 [81], Niinemets, 2002 [60]	**162**, 162, [143-180]	Zheng et al., 2002 [180], Niinemets, 2002 [143]
Scots pine	**87**, 83, [38-144]	Niinemets et al., 2001 [48], Niinemets, 2002 [83], Warren et al., 2003 [123], Jach & Ceulemans, 2000 [144], Wang, 1996 [38]	**219**, 237, [110-345]	Niinemets et al., 2001 [110], Niinemets, 2002 [237], Warren et al., 2003 [259], Jach & Ceulemans, 2000 [345], Wang, 1996 [146]
Mediterranean broadleaf evergreen	**56**		**97**	
Holm Oak	**56**, 50, [36-87]	Martin StPaul et al., 2012 [87], Niinemets, 2002 [36] & [40], Juárez-lópez, et al., 2008 [61]	**97**, 91, [59-139]	Martin StPaul et al., 2012 [139], Niinemets, 2002 [65] & [72], Juárez-lópez, et al., 2008 [110]
Mediterranean needleleaf evergreen	**56**		**97**	
Aleppo pine	No species specific data – use Holm Oak as surrogate			
Temperate Crops				
Wheat	180 [25-261]	Cf. Büker et al., 2007	400 [87-522]	Cf. Büker et al., 2007
Mediterranean Crops*	**48**	**Clark et al., 2011 [48]**	**105**	**(assuming Vcmax and Jmax ratio is same as Wheat at 2.2)**
Maize*	48	Clark et al., 2011 [48]	105	(assuming Vcmax and Jmax ratio is

		same as Wheat at 2.2)	
Root Crops	180 [25-261]	**See wheat**	400 [87-522]	**See wheat**
Potato	180 [25-261]	See wheat	400 [87-522]	See wheat
Vineyards	**100 [50-100]**	**Büker et al., 2007**	**225 [120-260]**	**Büker et al., 2007**
Grapevine	100 [50-100]	Büker et al., 2007	225 [120-260]	Büker et al., 2007
Grassland/Semi-natural/Med Scrub	**48**	**Clark et al., 2011 [48]**	**105**	**(assuming Vcmax and Jmax ratio is same as Wheat at 2.2)**

Table 2. Parameterisation of the DO3SE_C model –minimum stomatal conductance (g0, mol H_2O m^{-2} s^{-1}), the ratio of Vcmax:Jmax (where red denotes a ratio based on the mean values of Jmax and VCmax found in the literature as in Table 1) and species-specific composite sensitivity of gs to An (m),

Species / cover type	g0,	Ref	Vcmax:Jmax	Ref	m	Ref
Deciduous forest	**0.03**	**0.03**	**2**			
Birch	0.03	Büker et al., 2007	**2** 1.81, 1.76 [1.47-2.19]	Hayes (2014) Pers. Comm. [1.47], Rey & Jarvis, 1998 [2.19], Dreyer, et al., 2001 [1.76]	**8.6**	Hayes (2014) Pers. Comm. [8.6]
Beech	0.03	Büker et al., 2007	**2.05** 2.11, 1.95, [1.82-2.37]	Bader et al., 2010 [2.73], Löw et al., 2007 [1.82], Parelle et al., 2006 [1.96], Dreyer, et al., 2001 [1.94], Balandier et al., 2007 [2.37], Fleck, 2001 [1.83]	**8.6**	Birch value used as surrogate
Temperate oak	0.03	Use Beech value	**1.98** 2, 2.7, [1.73-3.0]	Marzuoli & Gerosa (2014) Pers. Comm. [1.82], Dreyer et al., 2001 [1.75] & [1.731], Bader et al., 2010 [3.00]	**8.6**	Birch value used as surrogate
Coniferous Forest			**2.4**		**9.2**	
Norway spruce	0.03	Use Beech value	**2.28** 2.3, 2.3, [2.22-2.38]	Zheng et al., 2002 [2.22], Niinemets, 2002 [2.38]	**9.2**	Nikolov & Zeller, 2003 [9.2]
Scots pine	0.03	Use Beech value	**2.52** 2.65, 2.40, [2.11-3.84]	Niinemets et al., 2001 [2.32], Niinemets, 2002 [2.86], Warren et al., 2003 [2.11], Jach & Ceulemans, 2000 [2.40], Wang, 1996 [3.84]	**9.2**	Nikolov & Zeller, 2003 [9.2]
Mediterranean broadleaf evergreen			**1.73**		**8.6**	
Holm Oak	0.03	Use Beech value	**1.73** 1.7, 2, [1.6-1.8]	Martin StPaul et al., 2012 [1.6], Juárez-lópez, et al., 2008 [1.8]	8.6	Birch value used as surrogate
Mediterranean			**1.73**		**8.6**	

needleleaf evergreen					
Aleppo pine	0.03	Use Beech value	No species specific data – use Holm Oak as surrogate		
Temperate Crops	**0.02**	**Büker et al., 2007**	**2.22**	**Büker et al., 2007**	**8.12**	**Büker et al., 2007**
Wheat	0.02	Büker et al., 2007	**2.22**	Büker et al., 2007	8.12	Büker et al., 2007
Mediterranean Crops*	**0.02**	**See wheat**	**2.22**	**Büker et al., 2007**	**8.12**	**Büker et al., 2007**
Maize*	0.02	See wheat	**2.22**	Büker et al., 2007	8.12	Büker et al., 2007
Root Crops	**0.02**	**See wheat**	**2.22**	**Büker et al., 2007**	**8.12**	**Büker et al., 2007**
Potato	0.02	See wheat	**2.22**	Büker et al., 2007	8.12	Büker et al., 2007
Vineyards	**0.05**	**See wheat**	**2.25**	**Büker et al., 2007**	**6.14**	**Büker et al., 2007**
Grapevine	0.05	Büker et al., 2007	**2.25**	Büker et al., 2007	6.14	Büker et al., 2007
Grassland/Semi-natural/Med Scrub	**0.02**	**See wheat**	**2.22**	**Büker et al., 2007**	**8.12**	**Büker et al., 2007**

DO$_3$SE fits into this scheme by providing a sophisticated approach to calculating stomatal fluxes, and therefore pollutant exchange with the vegetation, in each of the canopy layers. Stomatal conductance is calculated on a per-layer basis using both general meteorological data and per-layer values resulting from the dispersal model (e.g. CO$_2$ concentration) and other canopy-related effects (e.g. attenuation of sunlight).

Development of the Fortran coding of the ESX-DO$_3$SE model.
ESX can be described as a one-dimensional chemical transport model, working on a vertical grid, for a single land cover type. EMEP also has vertical transport within its larger 3-dimensional scheme, in addition to the large-scale horizontal grid and for several land covers per grid square. The EMEP model also uses several nested time intervals, most notably daily, 3-hourly, hourly and 20 minutes. As a smaller-scale model, ESX is run for every 20-minute interval, and every appropriate land cover, to solve the localised diffusion and chemical interactions. It is initialised with a starting state from the EMEP model's chemical concentrations data for the vertical range that ESX is being run for, and resulting fluxes are fed back to this data.
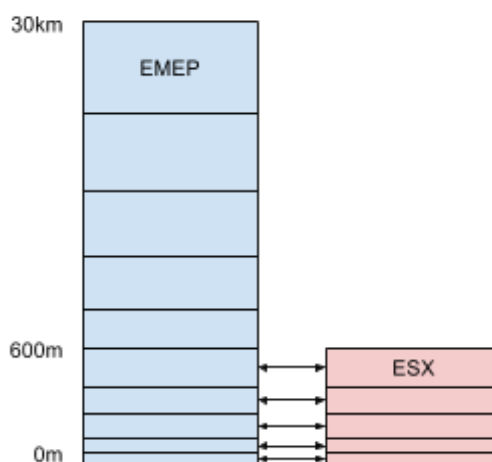
The existing code included much of the diffusion and chemical mechanism models (the latter being re-used from EMEP). A framework was created within which the various parts of the ESX-DO$_3$SE model could reside, i.e. the data flow between meteorological inputs, chemical concentrations, the diffusion model and DO$_3$SE's stomatal conductance model. An important aspect of this integration was to establish how to compromise on the design of both DO$_3$SE and ESX to allow ESX's version of DO$_3$SE to easily be updated with the most recent DO$_3$SE model developments without re-integration being a major undertaking each time changes were made to the DO$_3$SE model.

Similar considerations were needed to establish how to write ESX code that could be a standalone prototype but also be called from EMEP code. This required organising data variables within the model, grouping them where appropriate to give a coherent picture of flow within the model and making the code more maintainable. The DO$_3$SE model needed to be re-designed to allow it to be called from ESX code without hard-to-debug side-effects and without invoking aspects of the DO$_3$SE model that were in contradiction to the ESX model. This decoupling of DO$_3$SE methods from each other and the ESX model allowed improvements in this area to be tested within DO$_3$SE, ESX and EMEP with much less effort than before. This work has resulted in the production of a standalone ESX proof of concept model that could be driven by meteorological data, run a chemical interaction scheme and solve the diffusion model for vertical transport.

The integration of the new DO$_3$SE code into the ESX code has ensured that both multiplicative- and photosynthetic-based stomatal conductance methods to be configured and used by ESX. Code for the soil moisture part of the DO$_3$SE model was also integrated (for further details of this module see (Büker et al., 2012). Some additional work was required here to support the modelling of soil water

content within ESX. Since ESX was already using some code duplicated from EMEP, ESX was converted to a "sub-project" of EMEP's codebase and a lot of duplication was removed, this allows easier maintainability and integration with EMEP.

The EMEP model runs several nested time loops, and in the innermost loop, deposition is calculated for each land use category. As a starting point, we chose this part of the model to call ESX, driving it with the data available at this stage, and recording the results, without feeding them back into EMEP. This allows the behaviour of ESX to be analysed without introducing any feedback-driven anomalies.

References

Aphalo, P.J., & Jarvis, P. G. (1993). An analysis of Ball's empirical model of stomatal conductance. *Annals of Botany*, *72*, 312–327.

Bader, M. K.-F., Siegwolf, R., & Körner, C. (2010). Sustained enhancement of photosynthesis in mature deciduous forest trees after 8 years of free air CO(2) enrichment. *Planta*, *232*(5), 1115–25. doi:10.1007/s00425-010-1240-8

Balandier, P., Sinoquet, H., Frak, E., Giuliani, R., Vandame, M., Descamps, S., … Curt, T. (2007). Six-year time course of light-use efficiency, carbon gain and growth of beech saplings (Fagus sylvatica) planted under a Scots pine (Pinus sylvestris) shelterwood. *Tree Physiology*, *27*(8), 1073–1082. doi:10.1093/treephys/27.8.1073

Baldocchi, D. (1994). An analytical solution for coupled leaf photosynthesis and stomatal conductance models. *Tree Physiology*, *14*(7-8-9), 1069–1079. doi:10.1093/treephys/14.7-8-9.1069

Ball, J.T., Woodrow, I.E. Berry, J. A. (1987). A model predicting stomatal conductance and its contribution to the control of photosynthesis under different environmental conditions. In J. Biggens (Ed.), *Progress in photosynthesis research, Vol IV*. Dordrecht: Martinus Nijhoff.

Bernacchi, C. J., Singsaas, E. L., Pimentel, C., Portis Jr, a. R., & Long, S. P. (2001). Improved temperature response functions for models of Rubisco-limited photosynthesis. *Plant, Cell and Environment*, *24*(2), 253–259. doi:10.1046/j.1365-3040.2001.00668.x

Brooks, G.D., & Farquhar, A. (1985). Effect of temperature on the CO2/O2 specificity of ribulose-1,5-bisphosphate carboxylase/ oxygenase and the rate of respiration in light. *Planta*, *165*, 397–406.

Büker, P., Emberson, L. D., Ashmore, M. R., Cambridge, H. M., Jacobs, C. M. J., Massman, W. J., … de la Torre, D. (2007). Comparison of different stomatal conductance algorithms for ozone flux modelling. *Environmental Pollution (Barking, Essex : 1987)*, *146*(3), 726–35. doi:10.1016/j.envpol.2006.04.007

Clark, D. B., Mercado, L. M., Sitch, S., Jones, C. D., Gedney, N., Best, M. J., … Cox, P. M. (2011). The Joint UK Land Environment Simulator (JULES), model description – Part 2: Carbon fluxes and vegetation dynamics. *Geoscientific Model Development*, *4*(3), 701–722. doi:10.5194/gmd-4-701-2011

Collatz, G.J., Ball, J.T., Grivet, C. and Berry, J. A. (1991). Physiological and environmental regulation of stomatal conductance , photosynthesis and transpiration : a model that includes a laminar boundary layer *. *Agricultural and Forest Meteorology*, *54*(1074), 107–136.

Cox, P. M., Betts, R. a., Bunton, C. B., Essery, R. L. H., Rowntree, P. R., & Smith, J. (1999). The impact of new land surface physics on the GCM simulation of climate and climate sensitivity. *Climate Dynamics*, *15*(3), 183–203. doi:10.1007/s003820050276

Dreyer, E., Le Roux, X., Montpied, P., Daudet, F. A., & Masson, F. (2001). Temperature response of leaf photosynthetic capacity in seedlings from seven temperate tree species. *Tree Physiology*, *21*(4), 223–232. Retrieved from http://treephys.oxfordjournals.org/cgi/content/long/21/4/223

Farquhar, G.D., von Caemmerer, S., Berry, J. A. (1980). A biochemical model of photosynthetic CO_2 assimilation in leaves of C3 species. *Planta*, *149*, 78–90.

Fleck, S. (2001). Integrated analysis of relationships between 3D-structure , leaf photosynthesis , and branch transpiration of mature Fagus sylvatica and Quercus petraea trees in a mixed forest stand, (August).

Harley, P. C., Thomas, R. B., Reynolds, J. F., & Strain, B. R. (1992). Modelling photosynthesis of cotton grown in elevated CO_2. *Plant, Cell and Environment*, *15*(3), 271–282. doi:10.1111/j.1365-3040.1992.tb00974.x

Harley, P.C., Tenhunen, J.D., and Lange, O. L. (1986). Use of an analytical model to study limitations on net photosynthesis in Arbutus unedo under field conditions. *Oecologia*, *70*, 393–401.

Jach, M. E., & Ceulemans, R. (2000). Effects of season, needle age and elevated atmospheric CO_2 on photosynthesis in Scots pine (Pinus sylvestris). *Tree Physiology*, *20*(3), 145–157. doi:10.1093/treephys/20.3.145

Juárez-lópez, F. J., Escudero, A., & Mediavilla, S. (2008). Ontogenetic changes in stomatal and biochemical limitations to photosynthesis of two co-occurring Mediterranean oaks differing in leaf life span, (1980), 367–374.

Kosugi, Y., Shibata, S., Kobashi, S., & Caemmerer, V. (2003). Parameterization of the CO_2 and H_2O gas exchange of several temperate deciduous broad-leaved trees at the leaf, 285–301.

Leuning, R. (1990). MODELING STOMATAL BEHAVIOR AND PHOTOSYNTHESIS OF EUCALYPTUS-GRANDIS. *AUSTRALIAN JOURNAL OF PLANT PHYSIOLOGY*, *17*(2), 159–175.

Leuning, R. (1995). A critical appraisal of a combined stomatal-photosynthesis model for C3 plants. *Plant, Cell and Environment*, *18*(4), 339–355. doi:10.1111/j.1365-3040.1995.tb00370.x

Leuning, R. (2002). Temperature dependence of two parameters in a photosynthesis model. *Plant, Cell and Environment*, 1205–1210.

Löw, M., Häberle, K.-H., Warren, C. R., & Matyssek, R. (2007). O3 flux-related responsiveness of photosynthesis, respiration, and stomatal conductance of adult Fagus sylvatica to experimentally enhanced free-air O3 exposure. *Plant Biology (Stuttgart, Germany)*, *9*(2), 197–206. doi:10.1055/s-2006-924656

Martin StPaul, N.K., Limousin, J.-M., Rodríguez-calcerrada, J., Ruffault, J., Rambal, S., Letts, M.G., Misson, L. (2012). Photosynthetic sensitivity to drought varies among populations of Quercus ilex along a rainfall gradient. *Functional Plant Biology*, *39*(39), 25–37.

Martin, M J., Farage, P.K., Humphries, S.W., and Long, S. P. (2000). Australian Journal of Plant Physiology. *Australian Journal of Plant Physiology*, *27*, 211–219.

Medlyn, B. E., Dreyer, E., Ellsworth, D., Forstreuter, M., Harley, P. C., Kirschbaum, M. U. F., … Loustau, D. (2002). Temperature response of parameters of a biochemically based model of photosynthesis. II. A review of experimental data. *Plant, Cell and Environment*, *25*(9), 1167–1179. doi:10.1046/j.1365-3040.2002.00891.x

Medlyn, B. E., Duursma, R. a., Eamus, D., Ellsworth, D. S., Prentice, I. C., Barton, C. V. M., … Wingate, L. (2011). Reconciling the optimal and empirical approaches to modelling stomatal conductance. *Global Change Biology*, *17*(6), 2134–2144. doi:10.1111/j.1365-2486.2010.02375.x

Niinemets, U. (2002). Stomatal conductance alone does not explain the decline in foliar photosynthetic rates with increasing tree age and size in Picea abies and Pinus sylvestris. *Tree Physiology*, *22*(8), 515–535. doi:10.1093/treephys/22.8.515

Niinemets, U., Ellsworth, D. S., Lukjanova, a., & Tobias, M. (2001). Site fertility and the morphological and photosynthetic acclimation of Pinus sylvestris needles to light. *Tree Physiology*, *21*(17), 1231–1244. doi:10.1093/treephys/21.17.1231

Nikolov, T., Massman, W.J., & Schoettle, A. W. (1995). Coupling biochemical and biophysical processes at the leaf level : an equilibrium photosynthesis model for leaves of C 3 plants. *Ecological Modelling*, *80*, 205–235.

Parelle, J., Roudaut, J.P., Ducrey, M. (2006). Light acclimation and photosynthetic response of beech (Fagus sylvatica L .) saplings under artificial shading or natural Mediterranean conditions. *Annals of Forest Science*, *63*, 257–266. doi:10.1051/forest

Rey, A., & Jarvis, P. G. (1998). Long-term photosynthetic acclimation to increased atmospheric CO concentration in young birch (Betula pendula) trees, (1996).

Sellers, P. J., Berry, J. A., Collatz, G. J., Field, C. B., & Hall, F. G. (1992). Canopy reflectance, photosynthesis, and transpiration. III - A reanalysis using improved leaf models and a new canopy integration scheme. *Remote Sensing of Environment*, *42*(3), 187–216. Retrieved from http://linkinghub.elsevier.com/retrieve/pii/003442579290102P

Sellers, P.J., Randall. D.A., Collatz, G.J., Berry, J.A., Field, C.B., Dazlich, D.A., Zhang, C., Collelo, G.D. and Bounoua, L. (1996). A revised land surface parameterisation (SiB2) for atmospheric GCMs. Part I. Model formulation. *Journal of Climate*, *9*, 676–705.

Sharkey, T. D., Bernacchi, C. J., Farquhar, G. D., & Singsaas, E. L. (2007). Fitting photosynthetic carbon dioxide response curves for C(3) leaves. *Plant, Cell & Environment*, *30*(9), 1035–40. doi:10.1111/j.1365-3040.2007.01710.x

Su, H.-B., Paw U, K. T., & Shaw, R. H. (1996). Development of a coupled leaf and canopy model for the simulation of plant-atmosphere interaction. *Journal of Applied Meteorology*, *35*, 733–748. Retrieved from http://journals.ametsoc.org/doi/pdf/10.1175/1520-0450(1996)035<0733:DOACLA>2.0.CO;2

Von Caemmerer, S. & Farquhar, G. D. (1981). Some relationships between the biochemistry of photosynthesis and the gas exchange of leaves. *Planta*, *153*, 376–387.

Wang, K. (1996). Acclimation of photosynthetic parameters in Scats pine after three years exposure to elevated temperature and CO ,, *1923*(96).

Wang, Y., & Leuning, R. (1998). A two-leaf model for canopy conductance , photosynthesis and partitioning of available energy I : Model description and comparison with a multi-layered model. *Agricultural and Forest Meteorology*, *91*, 89–111.

Warren, C. R., Dreyer, E., & Adams, M. A. (2003). Photosynthesis-Rubisco relationships in foliage of Pinus sylvestris in response to nitrogen supply and the proposed role of Rubisco and amino acids as nitrogen stores, 359–366. doi:10.1007/s00468-003-0246-2

Wohlfahrt, G., Bahn, M., Haubner, E., Horak, I., Michaeler, W., Rottmar, K., … Cernusca, a. (1999). Inter-specific variation of the biochemical limitation to photosynthesis and related leaf traits of 30 species from mountain grassland ecosystems under different land use. *Plant, Cell and Environment*, *22*(10), 1281–1296. doi:10.1046/j.1365-3040.1999.00479.x

Wullschleger, S. D. (1993). Biochemical Limitations to Carbon Assimilation in C 3 Plants — A Retrospective Analysis of the j Curves from 109 Species. *Journal of Experimental Botany*, *44*(262), 907–920.

Zheng, D., Freeman, M., Bergh, J., Røsberg, I., & Nilsen, P. (2002). Production of Picea abies in South-east Norway in Response to Climate Change: A Case Study Using Process-based Model Simulation with Field Validation. *Scandinavian Journal of Forest Research*, *17*(1), 35–46. doi:10.1080/028275802317221064